Electronic Supplementary Material (ESI) for Organic & Biomolecular Chemistry.

SUPPORTING INFORMATION

Halogen bonding effect on electrochemical anion oxidation in Ionic Liquids.

Marie Alvarez,[a] Cedric Houzé,[a] Sihem Groni,[a] Bernd Schöllhorn*[a] and Claire Fave*[a]

[a] Laboratoire d'Electrochimie Moléculaire, UMR CNRS 7591, Université de Paris, 15 rue Jean-Antoine de Baïf, F-75205 Paris Cedex 13, France.

Contents

1. Syntheses and Characterization

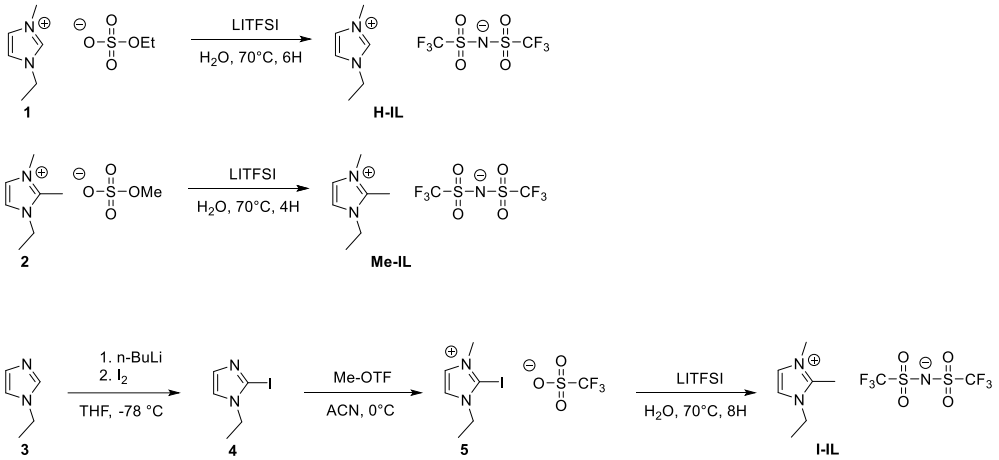

Scheme S1. General reaction scheme for the synthesis of 1-Ethyl-methylimisazolium bis(trifluoromethane)sulfonimide **(H-IL)**, 1-Ethyl-2,3-dimethylimidazolium bis(trifluoromethane)sulfonimide **(Me-IL)** and 1-Ethyl-2-iodo-3-methylimidazolium(bistrifluoromethane)sulfonimide **(I-IL)**.

1-Ethyl-methylimisazolium bis(trifluoromethane)sulfonimide (H-IL) [1]

1 (78 mmol, 1 eq) was diluted in 40 mL of water and then a solution of LiTFSI (87 mmol, 1.1 eq) in water (30 mL) was added. The solution was then heated to 70°C for 6 hours and stirred to obtain a homogeneous mixture. CH_2Cl_2 (70 mL) was then added to the aqueous solution. After extraction, the organic phase was dried over $MgSO_4$ and after evaporation a colorless liquid **H-IL** was obtained in 92% yield.

^{1}H NMR (400 MHz, CD_3CN) δ= 8.39 (s, 1H, N-C**H**-N), 7.37 (d, J = 2.1 Hz, 1H, N-C**H**-CH-N), 7.32 (d, J = 2.1Hz, 1H, N-CH-C**H**-N), 4.16 (q, J = 7.3 Hz, 2H, N-C**H**$_2$-CH_3), 3.81 (s, 3H, N-C**H**$_3$), 1.45 (t, J = 7.3 Hz, 3H, N-CH_2-C**H**$_3$).
^{13}C NMR (101 MHz, CD_3CN) δ= 137.0 (s, N-**C**H-N), 125.1 (s, N-**C**H-CH-N), 123.4 (s, N-CH-**C**H-N), 46.3 (s, N-**C**H_2-CH_3), 37.2 (s, N-**C**H_3), 15.6 (s, N-CH_2-**C**H_3).
^{19}F NMR (377 MHz, CD_3CN) δ= -80.2 (s, 6F, CF_3).

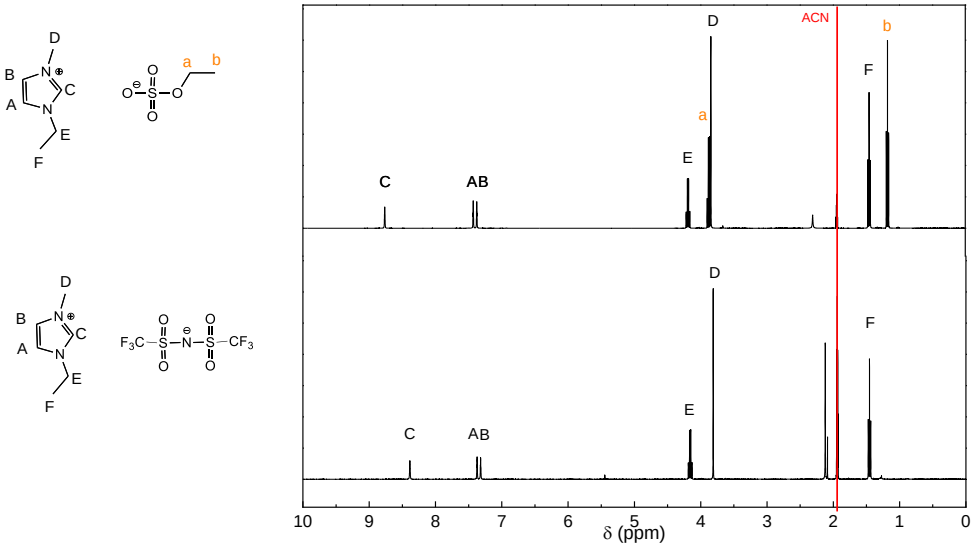

Figure S1 : ^{1}H NRM spectrum of **1** (up) and **H-IL** (Down) in CD_3CN-d_6.

1-Ethyl-2,3-dimethylimidazolium bis(trifluoromethane)sulfonimide (Me-IL) [1]

2 (78 mmol, 1 eq) was diluted in 50 mL of water and then a solution of LiTFSI (87 mmol, 1.1 eq) in water (50 mL) was added. The solution was then heated to 70°C for 4 hours and stirred to obtain a homogeneous mixture.

CH_2Cl_2 (70 mL) was then added to the aqueous solution. After extraction, the organic phase was dried over $MgSO_4$ and after evaporation a yellow liquid **Me-IL** was obtained in 89% yield.

^{1}H NMR (400 MHz, CD_3CN) δ= 7.26 (d, J = 2.1 Hz, 1H, N-C**H**-CH-N), 7.23 (d, J = 2.1 Hz, 1H, N-CH-C**H**-N), 4.07 (q, J = 7.3 Hz, 2H, N-C**H**$_2$-CH_3), 3.68 (s, 3H, N-C**H**$_3$), 2.49 (s, 3H, C-C**H**$_3$), 1.38 (t, J = 7.3 Hz, 3H, N-CH_2-C**H**$_3$).
^{13}C NMR (101 MHz, CD_3CN) δ= 145.7 (s, N-C-N), 123.8 (s, N-**C**H-CH-N), 121.6 (s, N-CH-**C**H-N), 44.9 (s, N-**C**H_2-CH_3), 36.0 (s, N-**C**H_3), 15.2 (s, C-**C**H_3), 10.2 (s, N-CH_2-**C**H_3).
^{19}F NMR (377 MHz, CD_3CN) δ= -80.2 (s, CF_3).

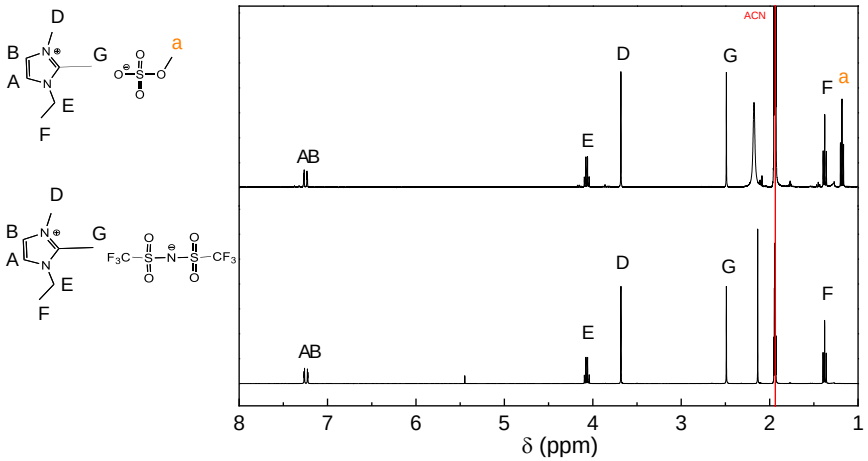

Figure S2 : ^{1}H NRM spectrum of **2** (up) and **Me-IL** (Down) in CD_3CN-d_6

1-Ethyl-2-iodoimidazole (4)[2]

1-Ethyl-imidazole **3** (0.10 mol, 1 eq) was dissolved in 200 mL of anhydrous THF at 0°C under Argon and agitation. A solution of BuLi at 1.6 M in hexane (0.13 mol, 1.25 eq) was then added drop by drop and shake for 1h30. Then a solution of I_2 (0.13 mol, 1.25 eq) in 15 mL THF anhydrous was carefully added at -78°C and then let it rise to room temperature and stir for 6 hours. The solvent was then evaporated and a saturated solution of sodium thiosulfate added. After extraction with CH_2Cl_2 and Flash chromatograph (Methanol/ CH_2Cl_2 (0.25/99.75)) the compound **4** was obtained as a yellow liquid and in 71.9% yield.

^{1}H NMR (400 MHz, CD_3CN) δ= 7.20 (s, 1H, N-C**H**-CH-N), 6.99 (s, 1H, N-CH-C**H**-N), 3.93 (q, J = 7.3 Hz, 2H, N-C**H**$_2$-CH_3), 1.33 (t, J = 7.3 Hz, 3H, N-CH_2-C**H**$_3$).
^{13}C NMR (101 MHz, CD_3CN) δ= 133.3 (s, N-**C**H-CH-N), 124.1 (s, N-CH-**C**H-N), 90.4 (s, N-**C**H_3), 45.6 (s, N-**C**H_2-CH_3), 16.4 (s, N-CH_2-**C**H_3).

1-Ehtyl-2-iodo-3-methylimidazolium triflate (5)[3]

Compound **4** (50 mmol, 1 eq) was dissolved in 100 mL of ACN and $CF_3SO_2OCH_3$ (77.5 mmol, 1.55 eq) was added at 0°C. The solution was stirred for 12 hours at room temperature. After evaporation of the solvent, the ionic liquid was washed twice with diethylether. The solvent was evaporated to give **5** in 42% yield.

^{1}H NMR (400 MHz, CD_3CN) δ= 7.62 (d, J = 2.1 Hz, 1H, N-C**H**-CH-N), 7.60 (d, J = 1.9 Hz, 1H, N-CH-C**H**-N), 4.15 (q, J = 7.3 Hz, 2H, N-C**H**$_2$-CH_3), 3.78 (s, 3H, N-C**H**$_3$), 1.41 (t, J = 7.3 Hz, 3H, N-CH_2-C**H**$_3$).
^{13}C NMR (101 MHz, CD_3CN) δ= 128.1 (s, N-**C**H-CH-N), 126.1 (s, N-CH-**C**H-N), 49.5 (s, N-**C**H_2-CH_3), 40.6 (s, N-**C**H_3), 15.3 (s, N-CH_2-**C**H_3)

1-Ethyl-2-iodo-3-methylimidazolium bis(trifluoromethane)sulfonimide (I-IL)

5 (25 mmol, 1 eq) was dissolved in 100 mL of water and then LiTFSI (31 mmol, 1.25 eq) was added. The solution was stirred for 8 hours at 70°C. After filtration, the ionic liquid was separated from aqueous solution and dried over $MgSO_4$. The light brown liquid **I-IL** is obtained in 68% yield.

^{1}H NMR (400 MHz, CD_3CN) δ= 7.60 (d, J = 2.1 Hz, 1H, N-C**H**-CH-N), 7.58 (d, J = 2.1 Hz, 1H, N-CH-C**H**-N), 4.15 (q, J = 7.3 Hz, 2H, N-C**H**$_2$-CH_3), 3.78 (s, 3H N-C**H**$_3$), 1.41 (t, J = 7.3 Hz, 3H, N-CH_2-C**H**$_3$).
^{13}C NMR (101 MHz, CD_3CN) δ= 128.1 (s, N-**C**H-CH-N), 126.1 (s, N-CH-**C**H-N), 49.5 (s, N-**C**H_2-CH_3), 40.7 (s, N-**C**H_3), 15.2 (s, N-CH_2-**C**H_3).
^{19}F NMR (377 MHz, CD_3CN) δ= -80.18 (s, CF_3).

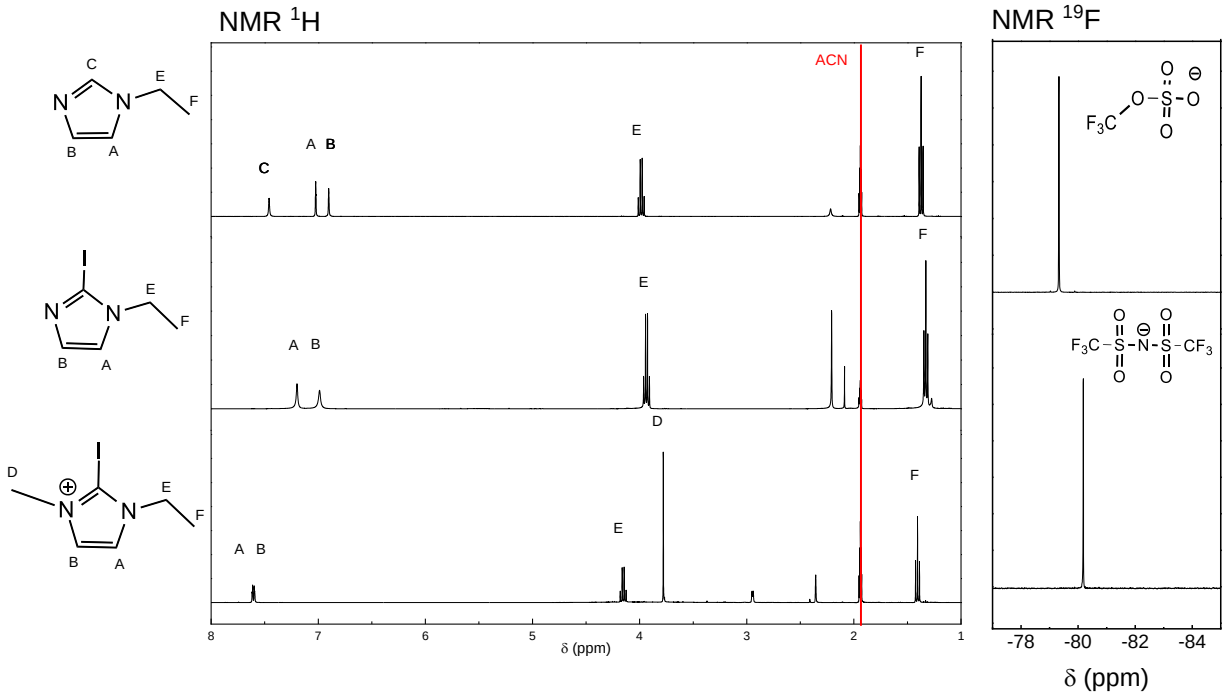

Figure S3 : Left: NMR ^{1}H spectrum superposition of **3** (Top), **4** (Middle) and **I-IL** (Bottom). Right: NMR ^{19}F spectrum superposition of **5** (Top) and **I-IL** (Bottom).

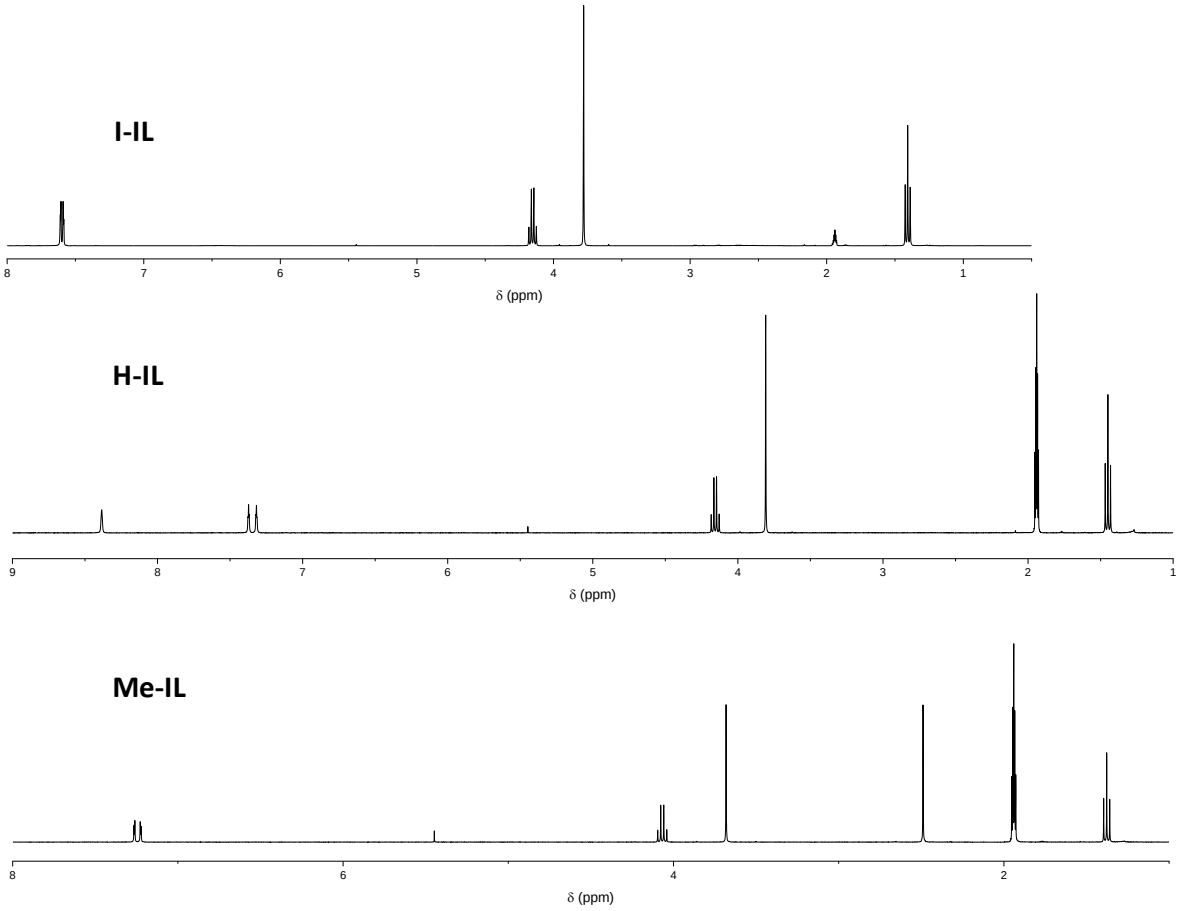

Figure S4 : NMR ^{1}H spectra in CD_3CN: superposition of the ILs **I-IL** (Top), **H-IL** (Middle) and **Me-IL** (Bottom)

2. Physicochemical Characterizations

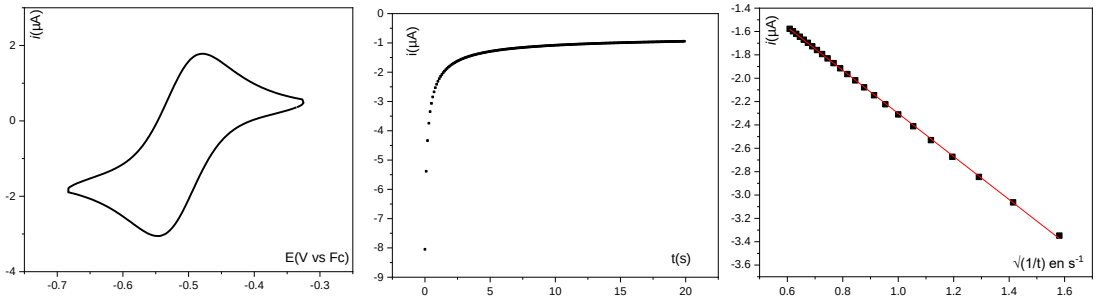

Figure S5: Left) CV of decamethylferrocene, dmfc (c = 4 mM) on glassy carbon electrode in **H-IL** at 40°C *vs* Fc, ν = 0.1V.s^{-1}. Middle) Chrono-amperometry at E_{app} = -0.61 V *vs* Fc for t = 20s. Right). Linear regression of $I(t) = nFAC\sqrt{D/\pi t}$ with I current (A), n number of electron (mol), F faraday constant (C.mol^{-1}) A electrode surface area (cm²), C concentration (mol.cm^{-3}) and D diffusion coefficient (cm².s^{-1}).

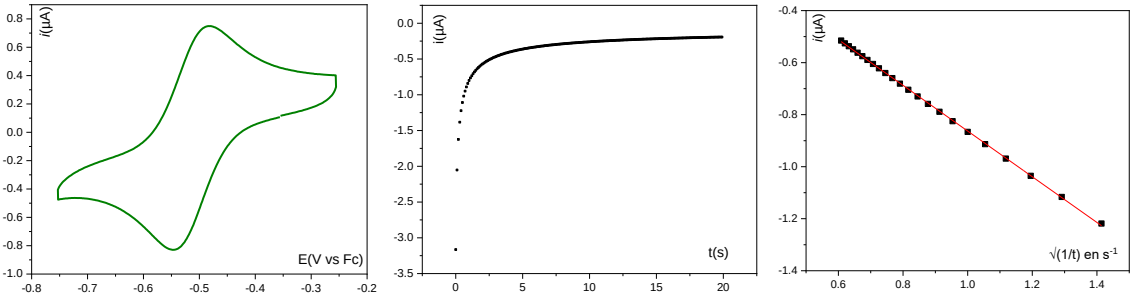

Figure S6: Left) CV of decamethylferrocene, dmfc (c = 3.5 mM) on glassy carbon electrode in **Me-IL** at 40°C *vs* Fc, ν = 0.1V.s^{-1}. Middle) Chrono-amperometry at E_{app} = -0.61 V *vs* Fc for t = 20s. Right) Linear regression of $I(t) = nFAC\sqrt{D/\pi t}$ with I current (A), n number of electron (mol), F faraday constant (C.mol^{-1}) A electrode surface area (cm²), C concentration (mol.cm^{-3}) and D diffusion coefficient (cm².s^{-1}).

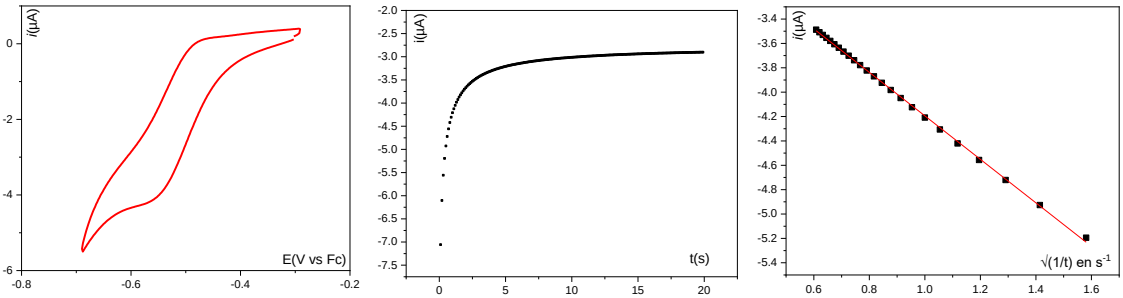

Figure S7: Left) CV of decamethylferrocene, dmfc (c = 5 mM) on glassy carbon electrode in **I-IL** at 60°C *vs* Fc, ν = 0.1V.s^{-1}. Middle) Chrono-amperometry at E_{app} = -0.61 V *vs* Fc for t = 20s. Right) Linear regression of $I(t) = nFAC\sqrt{D/\pi t}$ with I current (A), n number of electron (mol), F faraday constant (C.mol^{-1}) A electrode surface area (cm²), C concentration (mol.cm^{-3}) and D diffusion coefficient (cm².s^{-1}).

3. Electrochemical Characterization

4.1 when ILs are used as supporting electrolyte

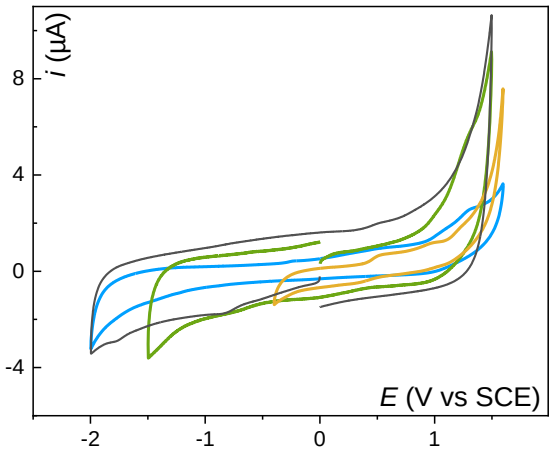

Figure S8: CV on glassy carbon electrode in DMF 40°C vs SCE, with 0.1 M $TBAPF_6$ (grey trace), 0.1 M **H-IL** (blue trace), 0.1 M **Me-IL** (green trace) and 0.1 M **I-IL** (orange trace). $\nu = 0.1 V.s^{-1}$.

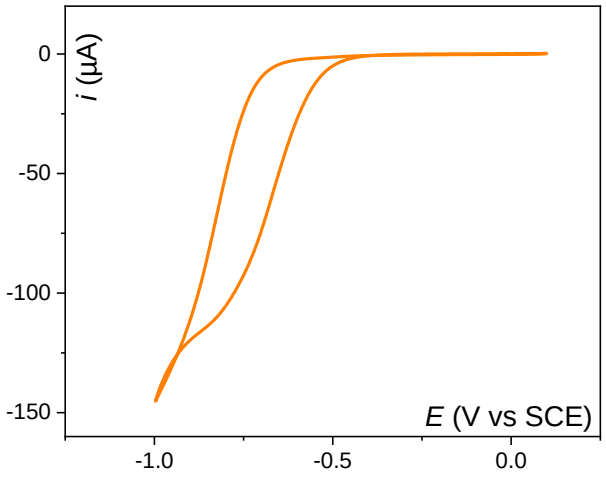

Figure 1

Figure S9: CV recorded on glassy carbon electrode in 0.1 M **I-IL** / DMF at 40°C. $\nu = 0.1 V.s^{-1}$.

4.2 when ILs are used pure

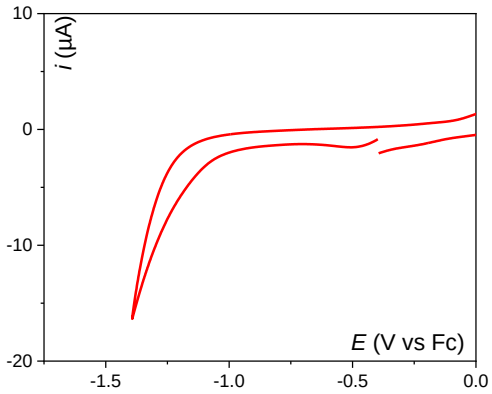

Figure S10: CV on glassy carbon of pure **I-Il** in reduction at 60°C; ν = 0.1 V.s^{-1} .

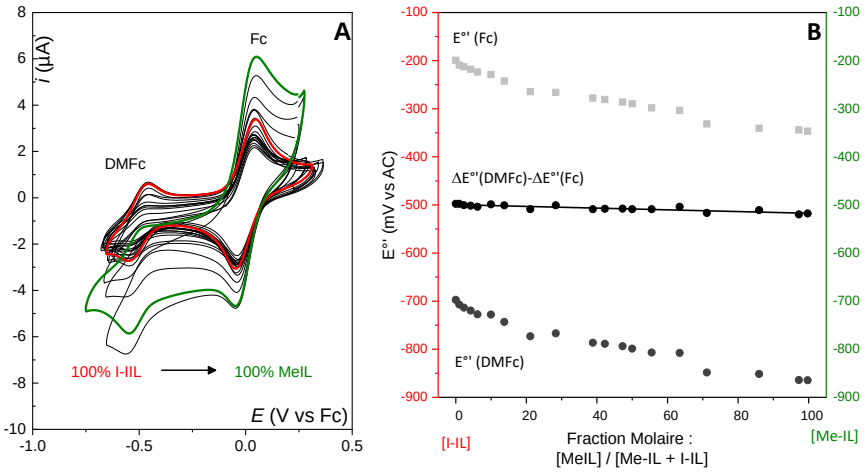

Figure S11: **A)** CV of Fc (3mM) and DMFc (1.6mM) at 60°C in **I-IL** (Red trace). Addition of **Me-IL** (Black trace) until a pure solution of **Me-IL** is obtained (Green trace). **B)** Standard potential of Fc (light Grey Square), DMFc (Dark Grey Circle), and as a function of **Me-IL** Molar fraction.

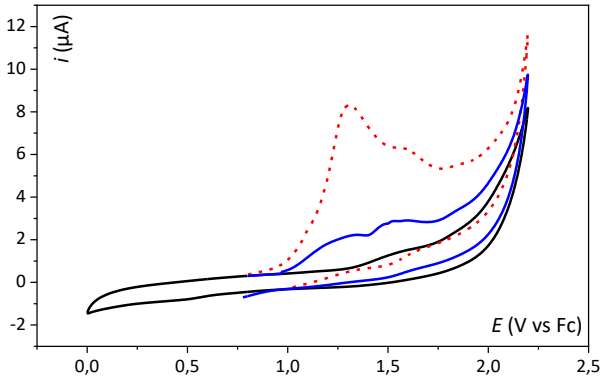

Figure S12 : CV on glassy carbon electrode in pure ionic liquids **I-IL** vs Fc, ν = 0.1 V.s$^{-1,}$ T = 60°C. **I-IL** (black trace), after 5s of electrolysis at E_{app} = 0.4 V vs Fc (blue trace), with addition of TBAI at c =1.5 mM in **I-IL** (red dot).

4. Single Crystal XRD

Single crystals were analyzed on a *Bruker* APEX-II with graphite monochromator, Cu K_α radiation from a microfocus sealed tube. The Structure was solved using the Olex2 software package in combination with ShelXL and ShelXT.[4,5] Pictures of the structures were generated with Diamond 4.[6]

Table S1. Crystal data and structure refinement for **[I-IL, I^-]**

Empirical formula	$2(C_6H_{10}IN_2)$, I_3, I
Formula weight [g/mol]	981,72
Crystal system	orthorhombic
Space group	-P 2ac 2ab
Lattice parameters [Å]	
a	15.7331(3)
b	13.3955(3)
c	23.5749(5)
α	90
β	90
γ	90
Volume [$Å^3$]	4968.5 (2)
Z, Z'	**Z**: 8 **Z'**:0
Temperature [K]	100(1)
Diffraction Device	XtaLAB Synergy, Dualflex, HyPix
Radiation Type	0.71073 Å (Mo K_a micro-focus sealed X-ray tube)

Table S2. Crystal data and structure refinement for **[I-IL, Br^-]**

Empirical formula	$C_6H_{10}IN_2$, Br
Formula weight [g/mol]	316.97
Crystal system	orthorhombic
Space group	-P 2ac 2ab
Lattice parameters [Å]	
a	11.7188(9)
b	11.8757(9)
c	13.5901(10)
α	90
β	90
γ	90
Density [g/cm^3]	2.226
Crystal size [mm^3]	0.270 x 0.240 x 0.110
Volume [$Å^3$]	1891.3(2)
Z, Z'	**Z**: 8 **Z'**:0
Temperature [K]	100(1)
Diffraction Device	XtaLAB Synergy, Dualflex, HyPix
Radiation Type	0.71073 Å (Mo K_a micro-focus sealed X-ray tube)

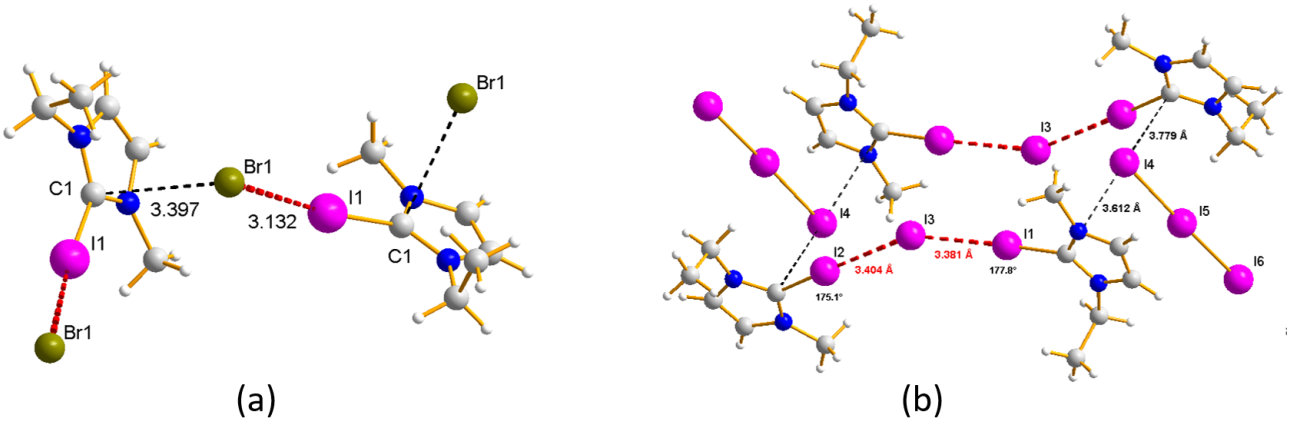

Figure S13: Short interatomic distances corresponding to non-covalent XB and π-anion interactions in compounds (a) **[I-IL, Br^-]** and (b) **[I-IL, I^-]**.

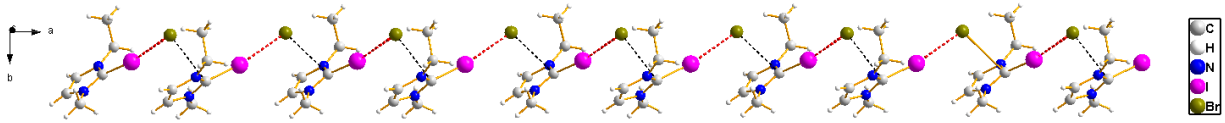

Figure S14: One-dimensional polymeric chain of **[I-IL, Br^-]** with alternating XB donor (I-IL+) and acceptor (Br-) units.

5. NMR Titration

For the NMR titrations 1 mM stock solutions of the hosts **Me-IL, H-IL, and I-IL,** as well as 100 mM guest (tetrabutylammonium chloride, bromide, iodide, nitrate and nitrophenoxide) solutions with 1mM of host were prepared in dry DMSO-D_6/HMDS (99.5/0.5 v/v). For each measurement, a single NMR tube was prepared by adding first the host, then the guest to the tube and, filling to an overall of 500 µL.

6.1 NMR titration with H-IL

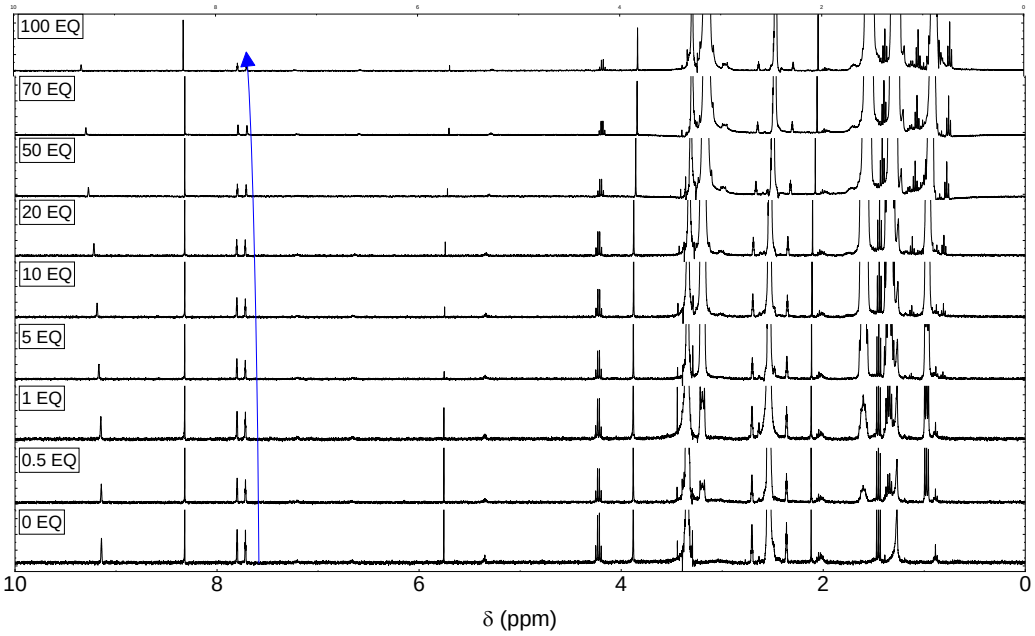

Figure S15: NMR spectra of titration of **H-IL** with Cl^- in DMSO. The blue trace indicates the shift of the signals of interest.

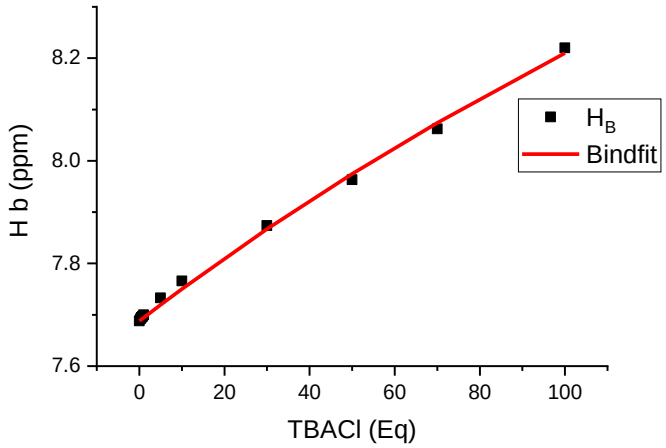

Figure S16: Variation of the NMR signal H_B as function of added equivalents of Chloride. The red curve was obtained by numerical simulation representing the best fit to the experimental data based on a 1 : 1 stoichiometry using Bindfit.

6.2 NMR titration with Me-IL

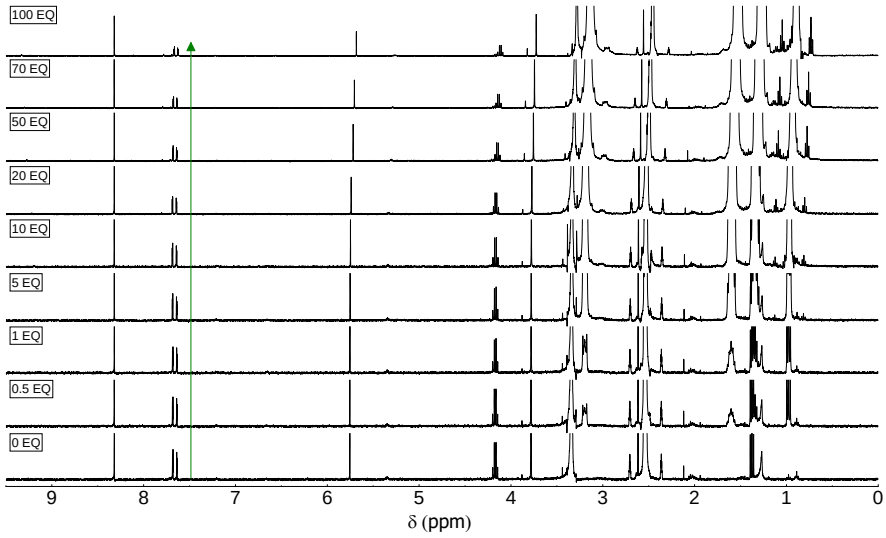

Figure S17: NMR spectra of titration of **H-IL** with Cl^- in DMSO. The green trace indicates the shift of the signals of interest.

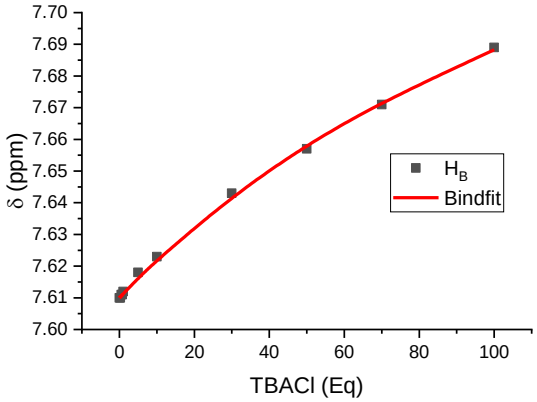

Figure S18: Variation of the NMR signal H_B as function of added equivalents of Chloride. The red curve was obtained by numerical simulation representing the best fit to the experimental data based on a 1 : 1 stoichiometry using Bindfit.

6.3 NMR titration with I-IL

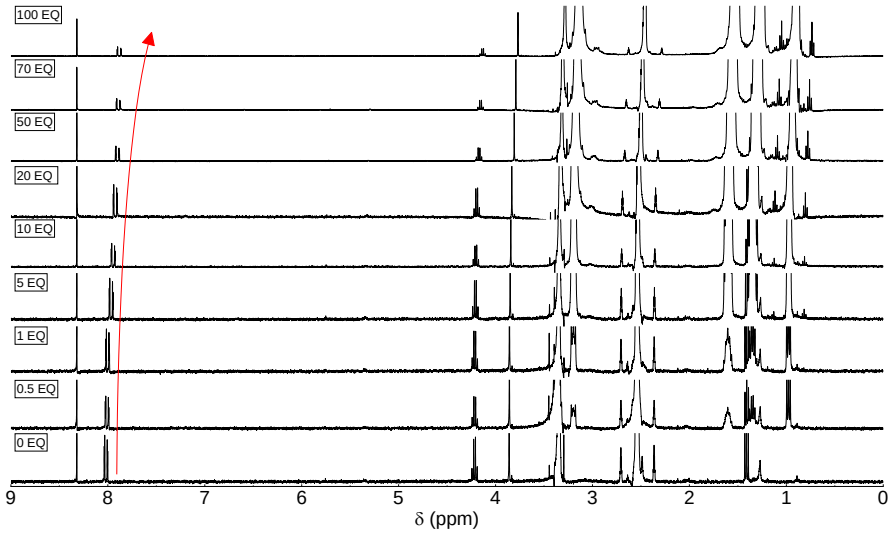

Figure S19: NMR spectra of titration of **I-IL** with Cl^- in DMSO. The red trace indicates the shift of the signals of interest.

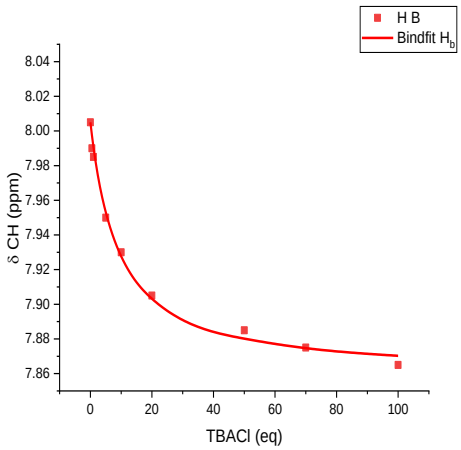

Figure S20: Variation of the NMR signal H_B as function of added equivalents of Chloride. The red curve was obtained by numerical simulation representing the best fit to the experimental data based on a 1 : 1 stoichiometry using Bindfit.

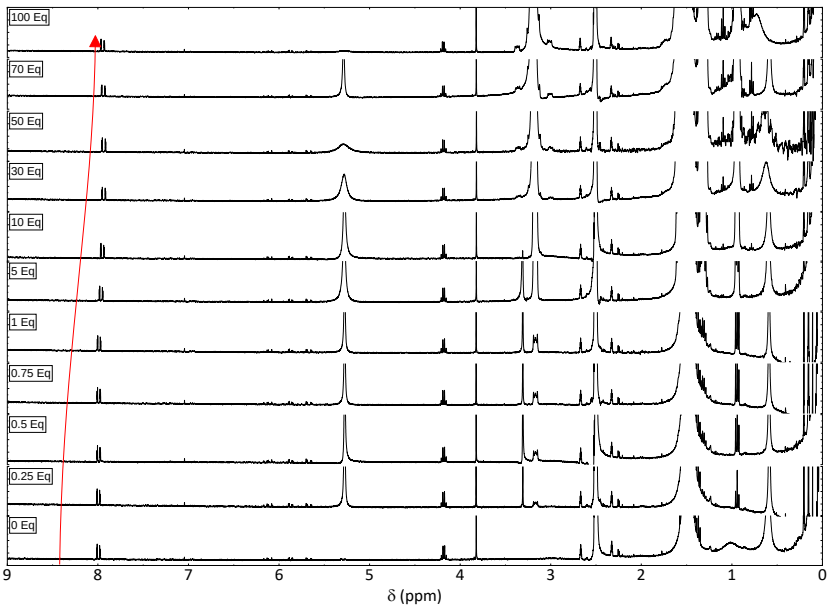

Figure S21: NMR spectra of titration of **I-IL** with Br^- in DMSO. The red trace indicates the shift of the signals of interest.

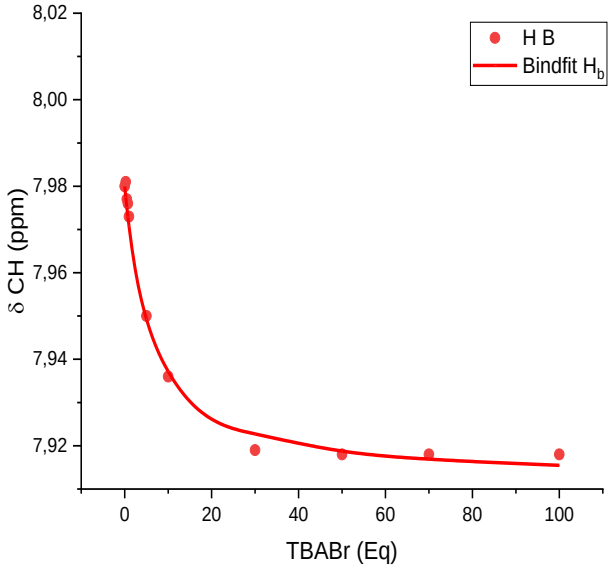

Figure S22: Variation of the NMR signal H_B as function of added equivalents of Bromide. The red curve was obtained by numerical simulation representing the best fit to the experimental data based on a 1 : 1 stoichiometry using Bindfit.

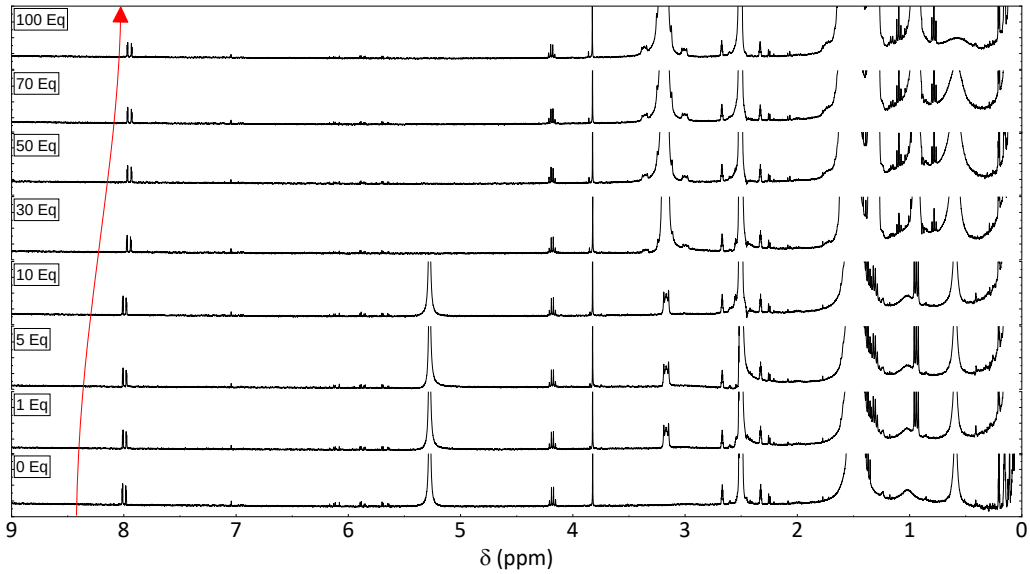

Figure S23: NMR spectra of titration of **I-IL** with I^- in DMSO. The red trace indicates the shift of the signals of interest.

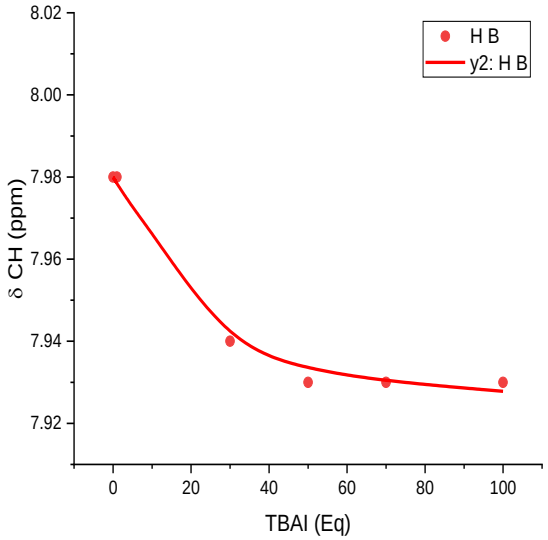

Figure S24: Variation of the NMR signal H_B as function of added equivalents of iodide. The red curve was obtained by numerical simulation representing the best fit to the experimental data based on a 1 : 1 stoichiometry using Bindfit.

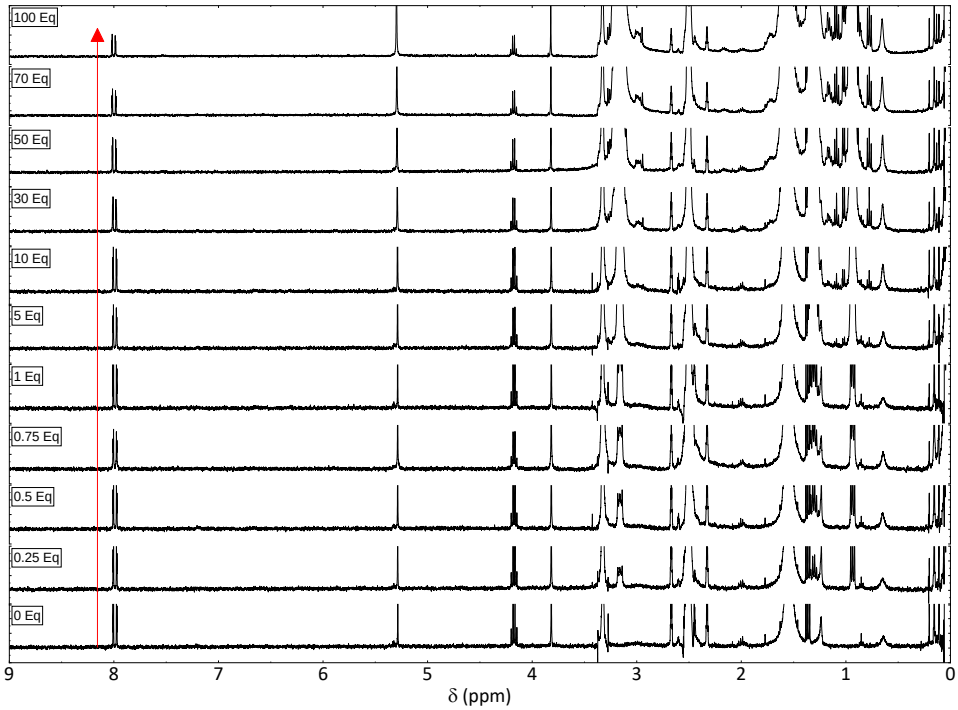

Figure S25: NMR spectra of titration of **I-IL** with NO_3^- in DMSO. The red trace indicates the shift of the signals of interest.

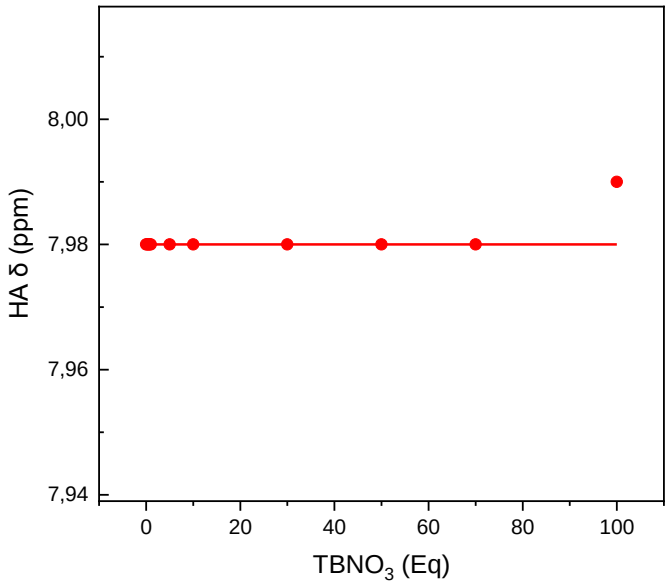

Figure S26 Variation of the NMR signal H_B as function of added equivalents of nitrate. The red curve was obtained by numerical simulation representing the best fit to the experimental data based on a 1 : 1 stoichiometry using Bindfit.

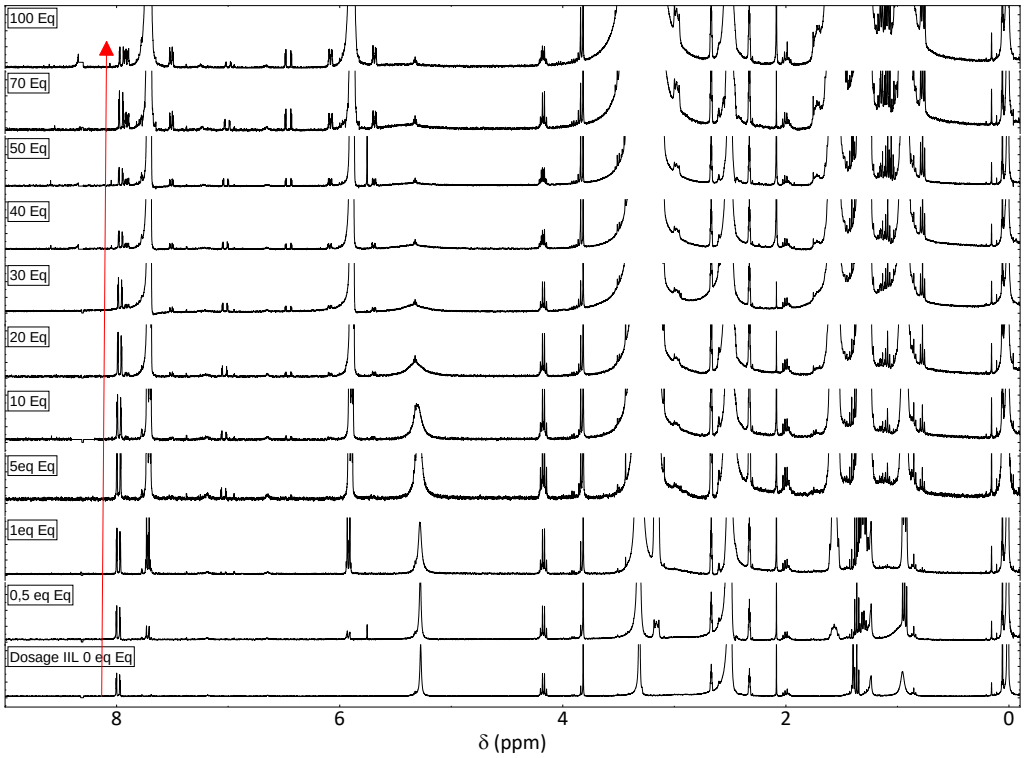

Figure S27: NMR spectra of titration of **I-IL** with NO_2PhO^- in DMSO. The red trace indicates the shift of the signals of interest.

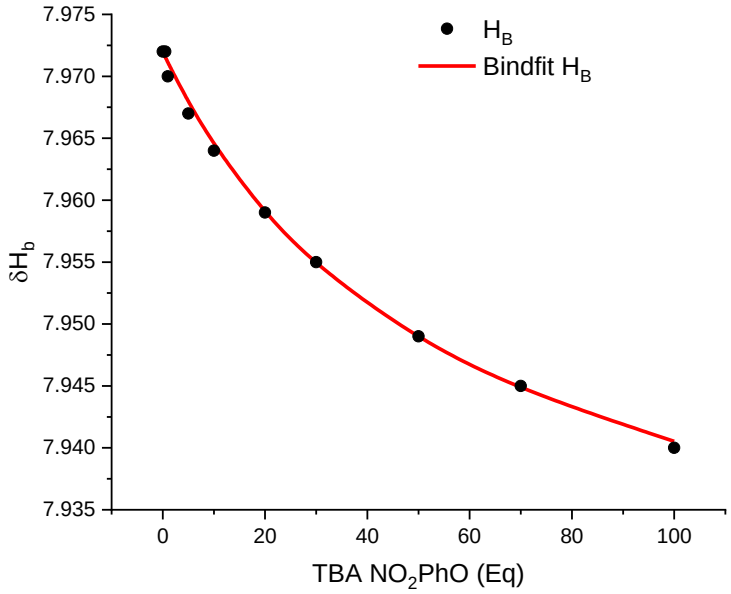

Figure S28: Variation of the NMR signal H_B as function of added equivalents of nitrophenolate. The red curve was obtained by numerical simulation representing the best fit to the experimental data based on a 1 : 1 stoichiometry using Bindfit.

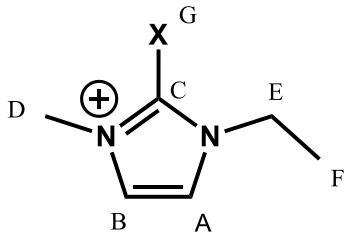

with X = H, Me or I

Table S2. NMR-titration table for (**Me-IL**, **H-IL**, **I-IL**) with **TBAX** (X = Cl, Br, I, NO_3, NO_2PhO) in DMSO/HMDS																	
									H-IL/Cl^-		**Me-IL**/Cl^-		**I-IL**/Cl^-	**I-IL/**Br^-	**I-IL**/I^-	**I-IL**/NO_3^-	**I-IL**/NO_2PhO^-
Tube Nr.	**V** [a]	**G/H**	V_{Host} [a]	V_{Guest} [a]	n_{Guest} [b]	n_{Host} [b]	c_{Host} [c]	c_{Guest} [c]	H_B	H_C	H_B	H_G	H_B	H_B	H_B	H_B	H_B
1	500	0	500	0	0.00	0.5	0.0010	0.0000	7.688	9.141	7.61	2.616	7.975	7.98	7.980	7.980	7.972
2	500	0.25	498.75	1.25	0.13	0.5	0.0010	0.0003	7.692	-	7.61	-	-	7.977	-	7.980	-
3	500	0.5	497.5	2.5	0.25	0.5	0.0010	0.0005	7.695	9.153	7.611	2.616	7.968	7.975	-	7.980	7.972
4	500	0.75	496.25	3.75	0.38	0.5	0.0010	0.0008	7.697	-	7.611	-	-	7.973	-	7.980	-
5	500	1	495	5	0.5	0.5	0.0010	0.0010	7.7	9.152	7.612	2.615	7.961	7.971	7.977	7.980	7.970
6	500	5	475	25	2.5	0.5	0.0010	0.0050	7.733	9.174	7.618	2.614	7.923	7.949	-	7.980	7.967
7	500	10	450	50	5	0.5	0.0010	0.0100	7.766	9.191	7.623	2.612	7.898	7.937	7.959	7.980	7.964
8	500	20	300	100	10	0.5	0.0010	0.0200	7.874	9.222	7.643	2.606	7.873	7.927	7.948	-	7.959
9	500	30	350	150	15	0.5	0.0010	0.0300	7.963	-	7.657	-	-	7.922	7.942	7.980	7.955
10	500	50	250	250	25	0.5	0.0010	0.0500	8.062	9.273	7.671	2.588	7.850	7.918	7.938	7.980	7.949
11	500	70	150	350	35	0.5	0.0010	0.0700	8.22	9.301	7.689	2.576	7.845	7.917	7.930	7.980	7.945
12	500	100	0	500	50	0.5	0.0010	0.1000	7.688	9.333	7.61	2.556	7.840	7.915	7.927	7.991	7.94

[a] in µL; [b] in µmol; [c] in M

6. Electrochemical behavior of Lewis Bases in ILs

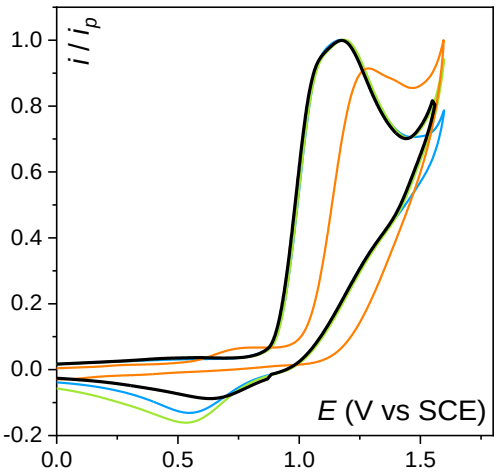

Figure S29: CV of TBACl (10 mM) in DMF with 0.1 M of various supporting electrolyte: **$TBAPF_6$** (black trace), **H-IL** (blue trace), **Me-IL** (green trace) and **I-IL** (orange trace). T = 40°C ; ν = 0.1 $V.s^{-1}$

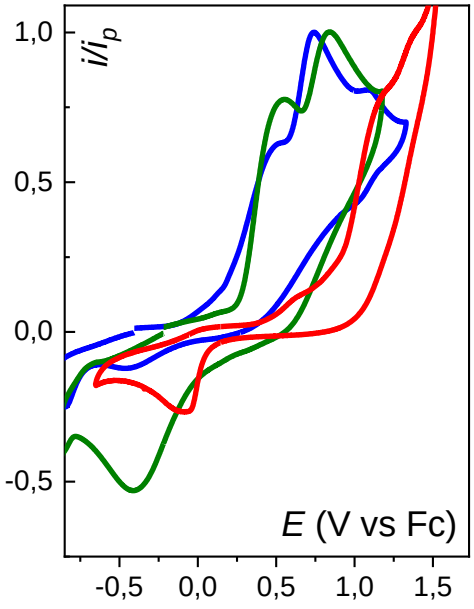

Figure S30: Normalised CV of TBABr (50 mM) on glassy carbon electrode in **H-IL** (blue trace) at 40°C, **Me-IL** (green trace) at 40°C, and **I-IL** (red trace) at 60°C. ν = 0.1 $V.s^{-1}$

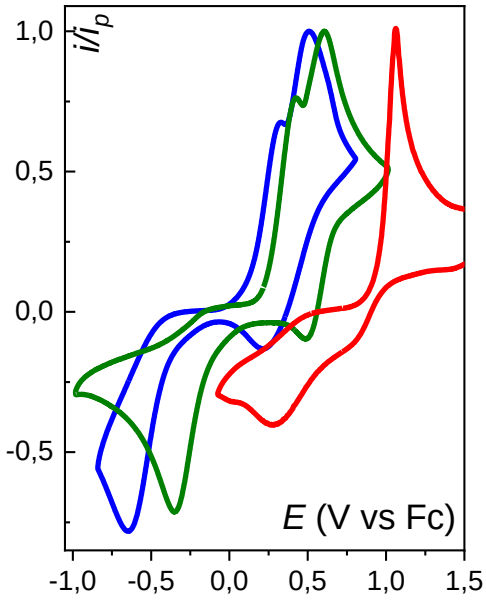

Figure S31: Normalised CV of TBAI (50 mM) on glassy carbon electrode in **H-IL** (blue trace) at 40°C, **Me-IL** (green trace) at 40°C, and **I-IL** (red trace) at 60°C. v = 0.1 V.s^{-1}

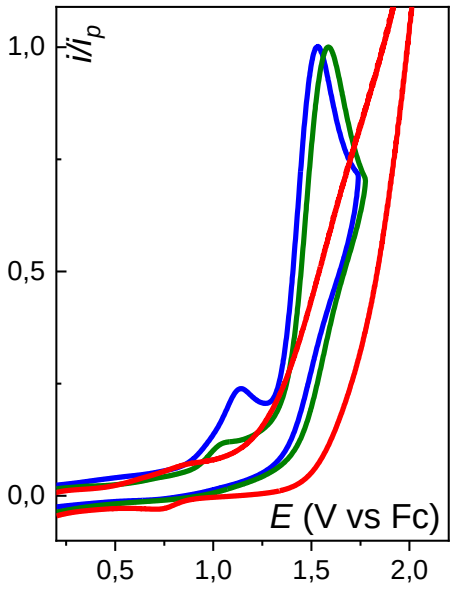

Figure S32: Normalised CV of $TBANO_3$ (50 mM) on glassy carbon electrode in **H-IL** (blue trace) at 40°C, **Me-IL** (green trace) at 40°C, and **I-IL** (red trace) at 60°C. ν = 0.1 V.s^{-1}

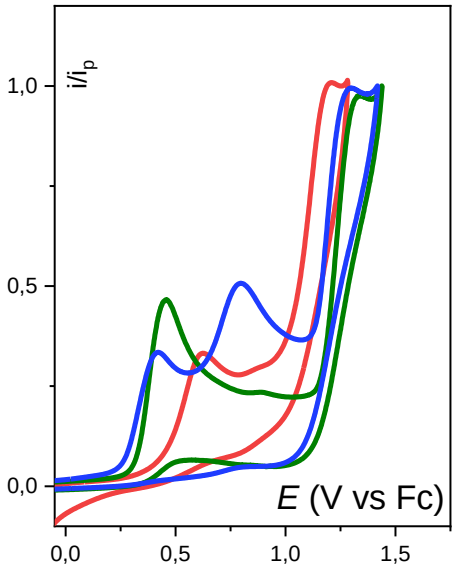

Figure S33: Normalised CV of $TBANO_2PhO$ (50 mM) on glassy carbon electrode in **H-IL** (blue trace) at 40°C, **Me-IL** (green trace) at 40°C, and **I-IL** (red trace) at 60°C. ν = 0.1 $V.s^{-1}$

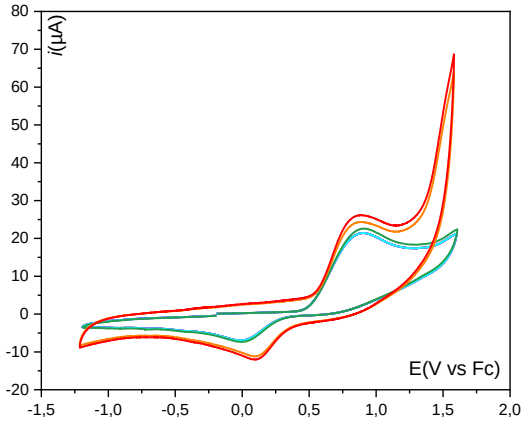

Figure S34: CV of Chloride (30 mM) on glassy carbon electrode in **Me-IL** (black trace) at 40°C, and after addition of H_2O, 0.2 (blue trace), 0.4 (pink trace), 0.6 (cyan trace), 1%wt (green trace), 1.6 (orange trace) and 2% wt (red trace). ν = 0.1 $V.s^{-1}$

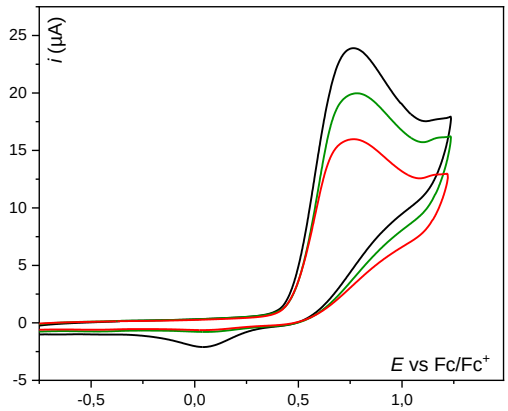

Figure S35: CV of Chloride (10 mM) on glassy carbon electrode in **H-IL** (black trace) at 40°C, and after addition of H_2O, 1%wt (green trace) and 2% wt (red trace). ν = 0.1 $V.s^{-1}$

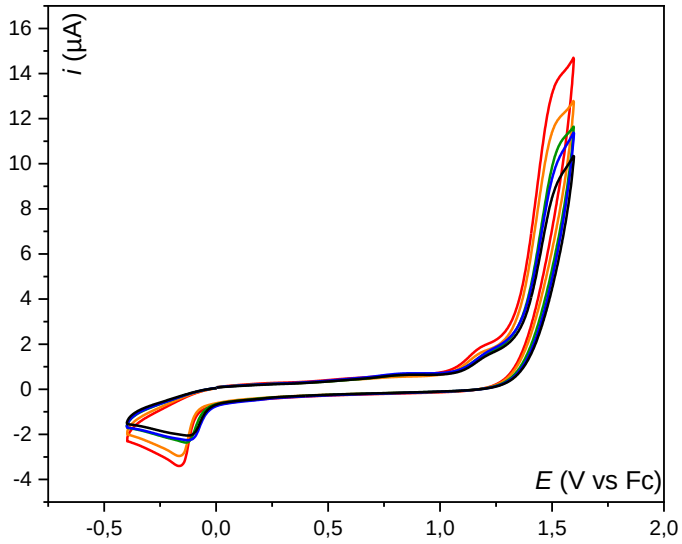

Figure S36: CV of Chloride (25 mM) on glassy carbon electrode in **I-IL** (black trace) at 60°C, and after addition of H_2O, 0.5%Wt (blue trace), 1%wt (green trace) 1.5%wt (orange trace) and 2% wt (red trace). ν = 0.1 V.s^{-1}

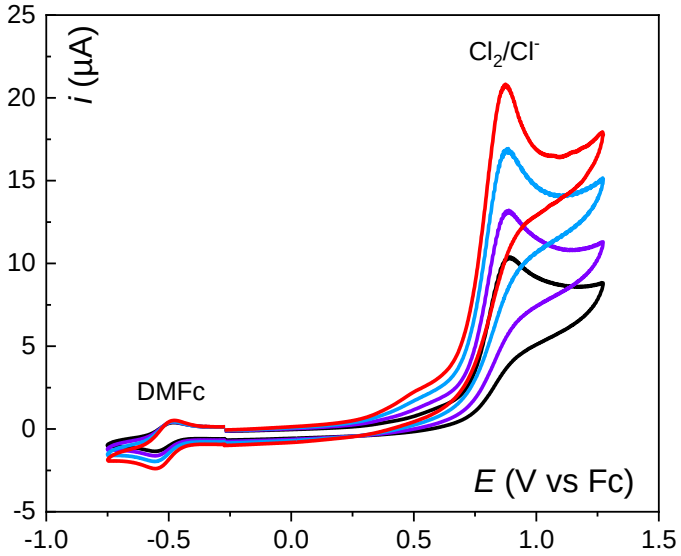

Figure S37: CV of Chloride (10 mM) on glassy carbon electrode in **Me-IL** (black trace) at 30°C, at 40°C (purple trace), at 50°C (blue trace) and 60°C (red trace) and after addition of H_2O 1%wt. ν = 0.1 V.s^{-1}

7. NMR spectra of commercially TBAX

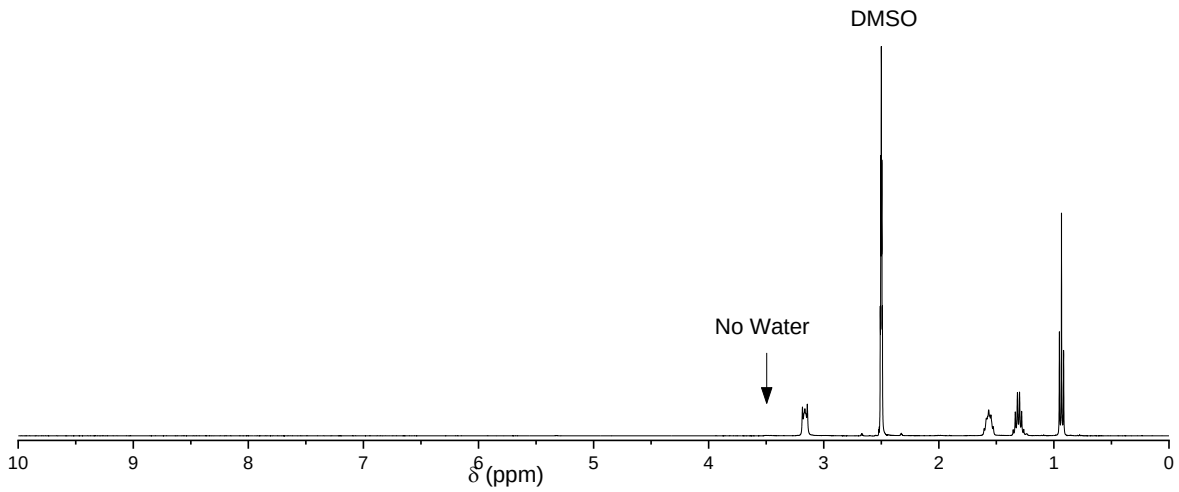

Figure S38: NMR spectra ^{1}H of titration Tetrabutylammonium chloride (TBACl) in DMSO-d_6

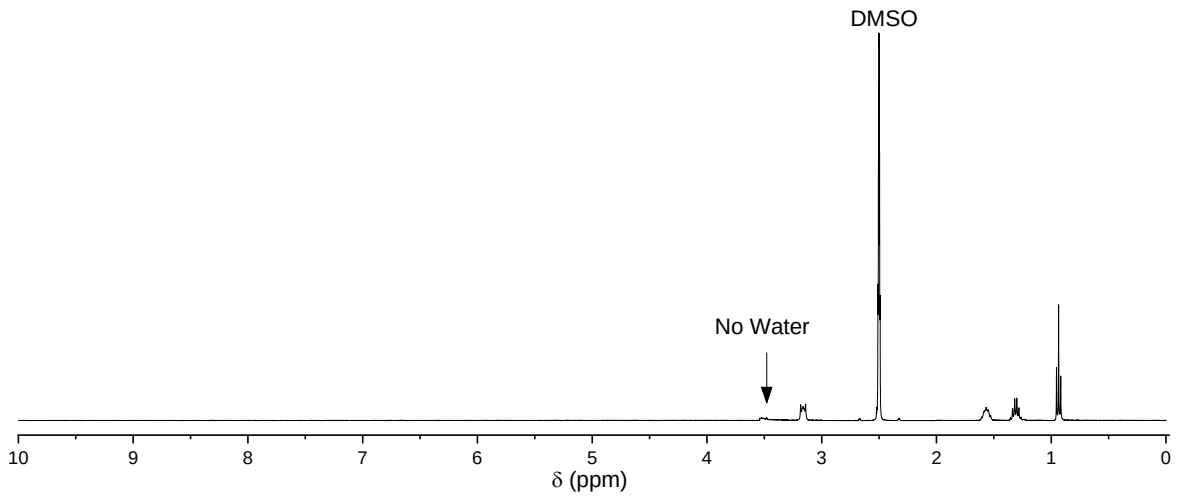

Figure S39: NMR spectra ^{1}H of titration Tetrabutylammonium bromide (TBABr) in DMSO-d_6

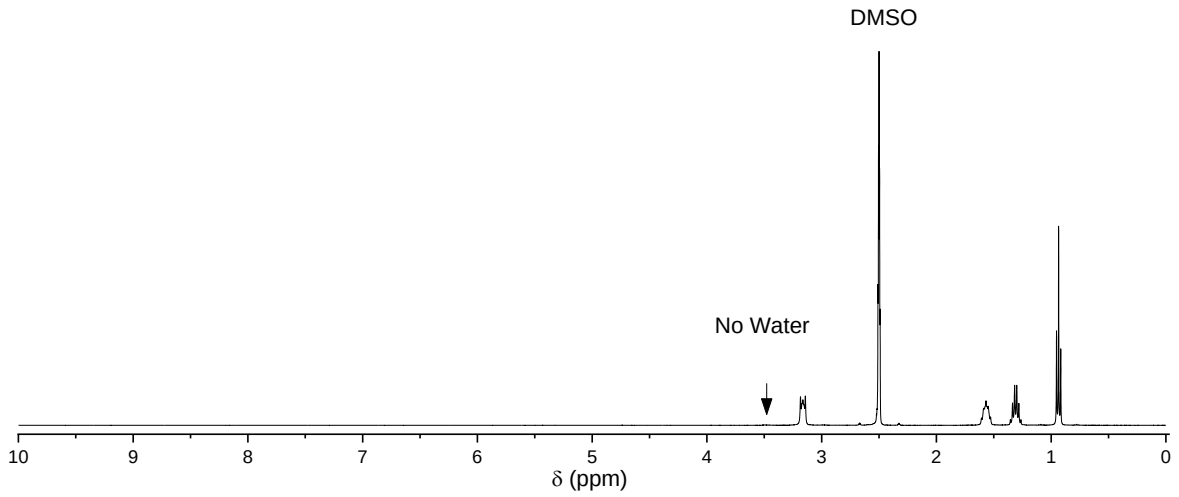

Figure S40: NMR spectra ^{1}H of titration Tetrabutylammonium iodide (TBAI) in DMSO-d_6

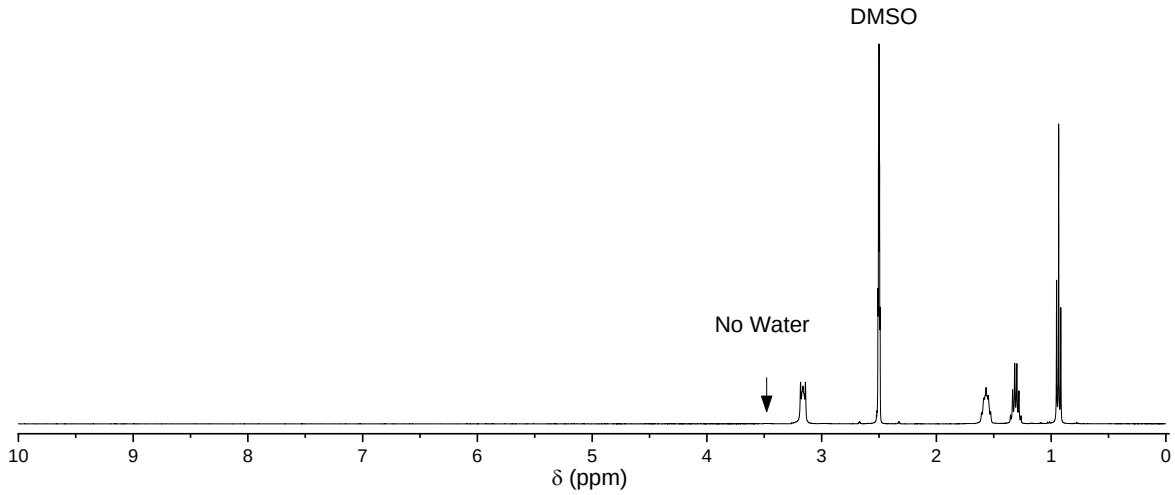

Figure S41: NMR spectra ^{1}H of titration Tetrabutylammonium nitrate ($TBANO_3$) in DMSO-d_6

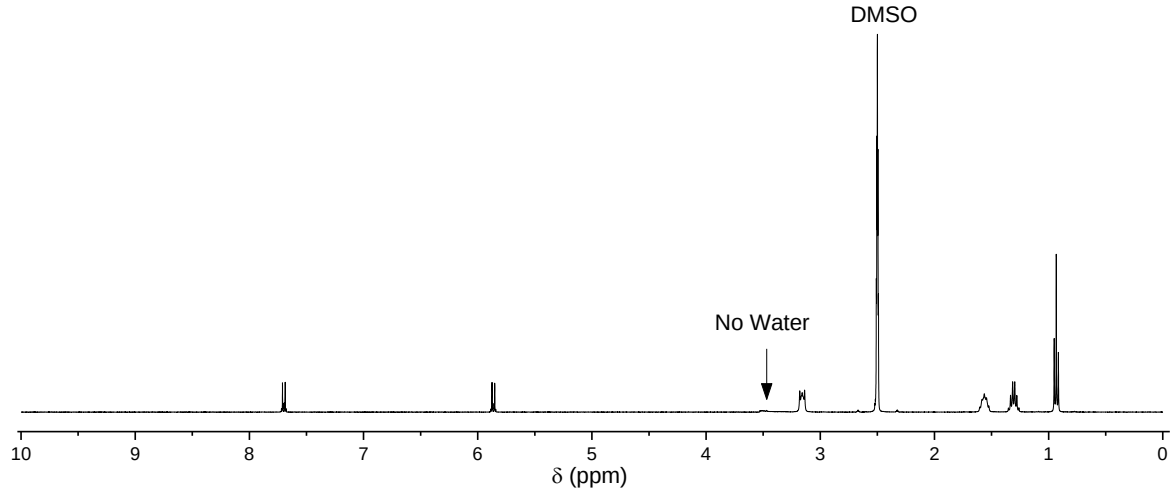

Figure S42: NMR spectra ^{1}H of titration Tetrabutylammonium p-Nitrophenoxide ($TBANO_2PhO$) in DMSO-d_6

8. References

[1] O. Fontaine, J. Ghilane, P. Martin, J.-C. Lacroix and H. Randriamahazaka, *Langmuir*, 2010, **26**, 18542–18549

[2] S. Chakraborty, R. Dutta and P. Ghosh, *Chem. Commun.*, 2015, **51**, 14793–14796

[3] J. M. Fraile, J. I. García, C. I. Herrerías, J. A. Mayoral, S. Gmough and M. Vaultier, *Green Chem*, 2004, **6**, 93–98.

[4] Sheldrick, G. M. A short history of SHELX. *Acta Crystallogr A Found Crystallogr* **2008**, *64*, 112–122, DOI: 10.1107/S0108767307043930.

[5] Hübschle, C. B.; Sheldrick, G. M.; Dittrich, B. ShelXle: a Qt graphical user interface for SHELXL. *J. Appl. Crystallogr.* **2011**, *44*, 1281–1284, DOI: 10.1107/S0021889811043202.

[6] Putz, H.; Brandenburg, K. *Diamond*; Crystal Impact: Bonn, Deutschland, 2014.